

Supplementary Information

All-inorganic 2D/3D $\text{Cs}_{x+2}\text{Pb}_{x+1}(\text{SCN})_2(\text{I}/\text{Br})_{3x+2}$ Perovskites

Tianyang Chen^{1†}, Shuangyan Hu^{2,3†}, Xuechang Zhou^{3*}, Jingshan Luo^{1*}

¹Institute of Photoelectronic Thin Film Devices and Technology, Solar Energy Research Center, Key Laboratory of Photoelectronic Thin Film Devices and Technology of Tianjin, Ministry of Education Engineering Research Center of Thin Film Photoelectronic Technology, Renewable Energy Conversion and Storage Center, Nankai University, Tianjin 300350, China

²Institute of Microscale Optoelectronics, Shenzhen University, Shenzhen 518060, China.

³College of Chemistry and Environmental Engineering, Shenzhen University, Shenzhen 518071, China

†These authors contribute equally to this work.

*Email: jingshan.luo@nankai.edu.cn; xczhou@szu.edu.cn

Methods

Materials. The SnO_2 colloid solution (tin (IV) oxide, 15% in H_2O colloidal dispersion) was purchased from Alfa Aesar. $\text{Pb}(\text{SCN})_2$ was purchased from Sigma-Aldrich. $\text{Pb}(\text{Ac})_2$, CsI , CsBr , lead bromide (PbBr_2) and lead iodide (PbI_2 , 99.99%) were purchased from Xi'an Polymer Light Technology Corp. 4-tert-butylpyridine (tBP, 96%), Bis(trifluoromethane) sulfon imide lithium salt (Li-TFSI, 99.95%), chlorobenzene (CB, 99.8%), isopropanol (IPA, 99.8%), dimethylsulfoxide (DMSO, 99.9%) were purchased from Sigma-Aldrich. 2,2',7,7'-tetrakis-(N, N-di-pmethoxyphenylamine)-9,9'-spirobifluorene (Spiro-OMeTAD) ($\geq 99.5\%$) was received from Youxuan. hexadecyltrimethylammonium iodide (CTAI) was purchased from Shanghai Bio. All chemicals were used as received without any other refinement.

Preparation of perovskite precursor solutions.

We prepared the 1M $\text{Cs}_{x+2}\text{Pb}_{x+1}(\text{SCN})_2\text{I}_{3x+2}$ ($x = 0, 1, 2, 3$) precursor solutions, 1M $\text{Cs}_{x+2}\text{Pb}_{x+1}(\text{SCN})_2\text{I}_{3x+2}-0.1\text{Pb}(\text{Ac})_2$ ($x = 0, 1, 2, 3$) precursor solutions, 0.5M $\text{Cs}_{x+2}\text{Pb}_{x+1}(\text{SCN})_2(\text{I}/\text{Br})_{3x+2}$ ($x = 3$) (I:Br = 1:0, 0.75:0.25, 0.5:0.5, 0.25:0.75, 0:1) precursor solutions and 0.5M $\text{Cs}_{x+2}\text{Pb}_{x+1}(\text{SCN})_2\text{Br}_{3x+2}$ ($x = 0, 1, 2, 3$) precursor solutions. The precursor chemicals were mixed stoichiometrically with anhydrous dimethyl sulfoxide (DMSO, ACROS, 99%) solvent and heated at 60°C until completely dissolved.

Device fabrication: The ITO substrate was cleaned by sequential sonication in detergent, deionized water, acetone, and ethanol for 10 min, respectively, with drying under airflow. The SnO_2 nanoparticle film was prepared by spin-coating a filtered and dispersed SnO_2 colloid solution (SnO_2 aqueous colloidal: deionized water = 1: 3) at 4000 rpm for 30 s on the clean ITO substrate with 10 min plasma cleaner treatments, and then annealing on a hot plate at 180°C for 30 min. The perovskite films were prepared by spin-coating the perovskite precursor solutions in a two-step program at

1000 rpm and 3000 rpm for 10 s and 50 s, respectively, on the glass/ITO/SnO₂ substrates, then annealing at 80 °C for 2 min. With the passivated devices, CTAI (2mg/ml in isopropanol) was spin-coated on perovskite film at 4000 rpm for 20 s. Hole-transporting layer was prepared by spin-coating the spiro-OMeTAD chlorobenzene solution (90 mg ml⁻¹) with 20.6 μl bis (trifluoromethane) sulfonimide lithium salt (Li-TFSI, Sigma-Aldrich, 520 mg ml⁻¹ in acetonitrile) and 35.5 μl 4-*tert*-butylpyridine (*t*-BP, Sigma-Aldrich) at 4,000 rpm for 30 s on top of the perovskite film. The devices were put into a dry-air glovebox (RH < 5%) for 12 h. Finally, an 80 nm gold electrode was deposited by thermal evaporation under a vacuum of $\sim 2 \times 10^{-5}$ Pa.

Characterizations

Material characterization: The top-view and cross-sectional morphologies of perovskite films were characterized by scanning electron microscopy (JEOL JSM-7800F). Optical absorption spectra were acquired using a UV-Vis-NIR spectrophotometer (Cary 5000). Steady-state photoluminescence (PL) spectra were performed with a PL spectrometer (Edinburgh Instruments, FS5) with an excitation at 475 nm.

Device characterization: Photocurrent density–voltage (J – V) curves were measured by a Keithley 2400 source with a solar simulator (HAL-320, Asahi Spectra Co. Ltd., Japan) to give the corresponding current response with a scan rate of 10 mV/s (the voltage step is 5 mV with a delay time of 50 ms). The light intensity was calibrated by a silicon photodiode. Cells were covered by a black metal mask with an active area of 0.067 cm². Short power output (SPO) was also carried on this system with a bias of the voltage at the maximum power point. Incident photon-to-current conversion efficiency (IPCE) was conducted in the air without encapsulation by an external quantum efficiency measurement system (TLS-300XU, Newport).

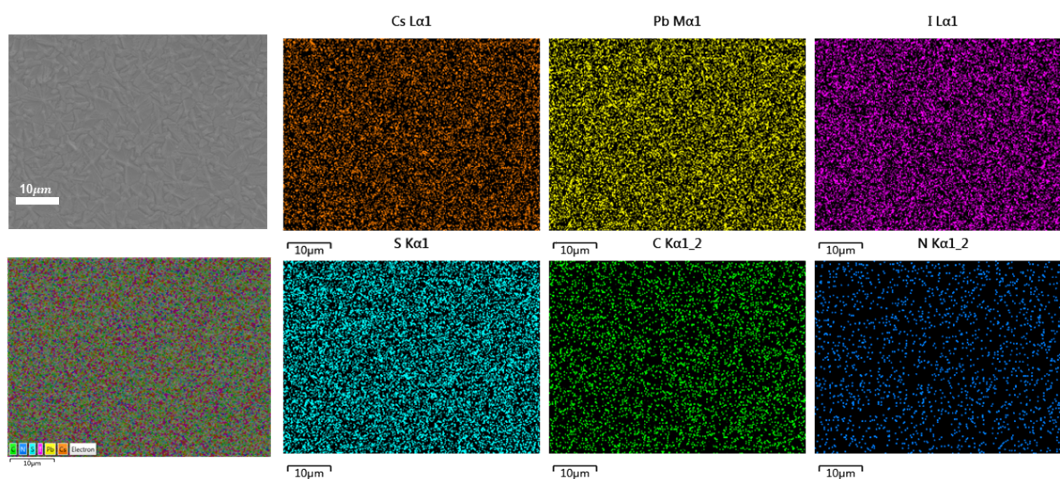


Figure S1. EDS of $\text{Cs}_{x+2}\text{Pb}_{x+1}(\text{SCN})_2\text{I}_{3x+2}$ ($x = 3$) films with $\text{Pb}(\text{Ac})_2$ additive.

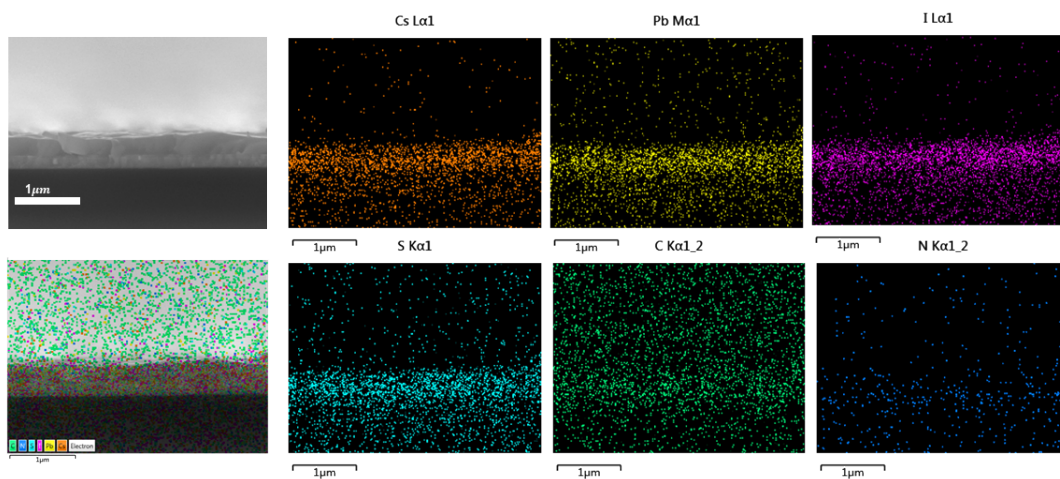


Figure S2. Cross-sectional EDS of $\text{Cs}_{x+2}\text{Pb}_{x+1}(\text{SCN})_2\text{I}_{3x+2}$ ($x = 3$) films with $\text{Pb}(\text{Ac})_2$ additive.

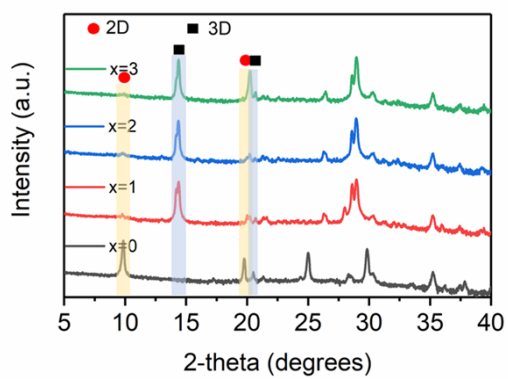


Figure S3. The XRD patterns of $\text{Cs}_{x+2}\text{Pb}_{x+1}(\text{SCN})_2\text{I}_{3x+2}$ films with $\text{Pb}(\text{Ac})_2$ additive ($x = 0, 1, 2, 3$).

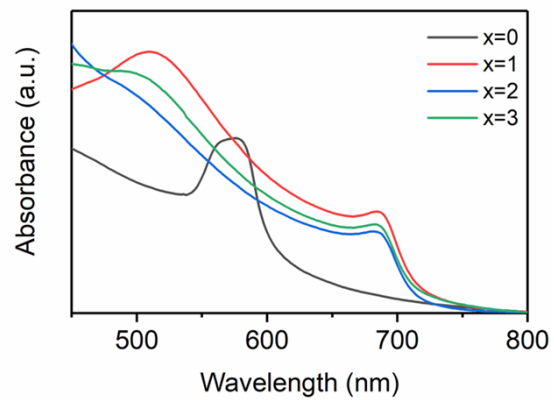


Figure S4. The UV-vis absorbance of Cs_{x+2}Pb_{x+1}(SCN)₂I_{3x+2} films with the Pb(Ac)₂ additive (x = 0, 1, 2, 3).

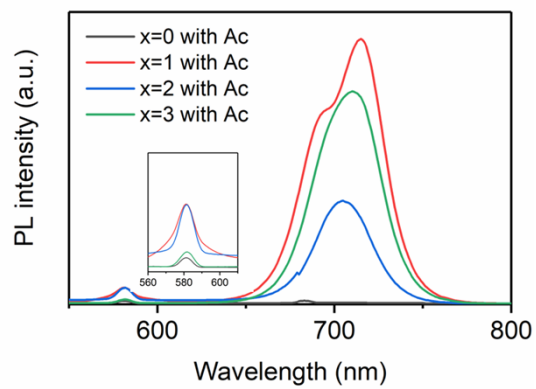


Figure S5. The steady PL spectra of $\text{Cs}_{x+2}\text{Pb}_{x+1}(\text{SCN})_2\text{I}_{3x+2}$ films with the $\text{Pb}(\text{Ac})_2$ additive ($x = 0, 1, 2, 3$).

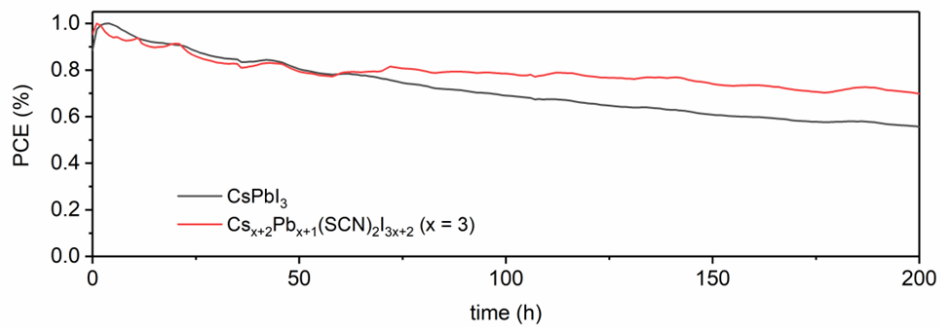


Figure S6. The maximum power point stability tracking of Cs_{x+2}Pb_{x+1}(SCN)₂I_{3x+2} (x = 3) and CsPbI₃ devices at room temperature under simulated AM1.5G 1-sun illumination. The Cs_{x+2}Pb_{x+1}(SCN)₂I_{3x+2} (x = 3) and CsPbI₃ devices are fabricated based on the same method. The initial efficiency of Cs_{x+2}Pb_{x+1}(SCN)₂I_{3x+2} (x = 3) and CsPbI₃ devices are 7.2% and 5.6%.

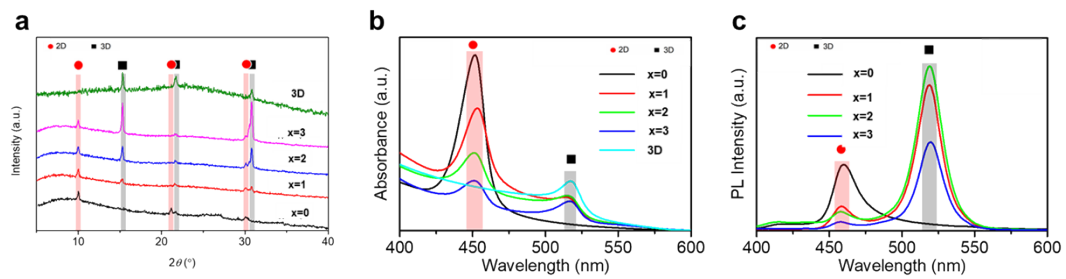


Figure S7. Basic properties of $\text{Cs}_{x+2}\text{Pb}_{x+1}(\text{SCN})_2\text{Br}_{3x+2}$ ($x = 0, 1, 2, 3$). a) The XRD patterns b) UV-vis absorbance c) steady PL spectra of $\text{Cs}_{x+2}\text{Pb}_{x+1}(\text{SCN})_2\text{Br}_{3x+2}$ ($x = 0, 1, 2, 3$).

Table S1. Device performance from JV curves and the integrated photocurrent density from EQE for the devices based on $\text{Cs}_{x+2}\text{Pb}_{x+1}(\text{SCN})_2\text{Br}_{3x+2}$ ($x = 0, 1, 2, 3$) films with $\text{Pb}(\text{Ac})_2$ additive and the $\text{Cs}_{x+2}\text{Pb}_{x+1}(\text{SCN})_2\text{Br}_{3x+2}$ ($x = 3$) films with $\text{Pb}(\text{Ac})_2$ additive and CTAI passivation.

Name	J_{sc} (mA/cm^2)	V_{oc} (V)	FF (%)	PCE (%)	Integrated J_{sc} (mA/cm^2)
x=0_RS	0.6	0.31	29.29	0.05	0.62
x=1_RS	2.24	0.77	17.13	0.29	1.98
x=2_RS	9.24	0.85	26.61	2.09	8.83
x=3_RS	12.99	0.86	54.88	6.15	11.99
x=3_CTAI_RS	13.2	0.99	61.66	8.1	
x=3_CTAI_RS	12.6	0.94	54.38	6.4	